

kde na levých stranách jsou šířky difrakčních linií po korekci na přístrojové rozšíření. Rovnice (4) a (5) tvoří soustavu dvou rovnic o dvou neznámých, D a e . Řešením této soustavy dostáváme pro velikost částic

$$D = \frac{1 \sec_1 \tan_2 + 2 \sec_2 \tan_1}{1 \tan_2 + 2 \tan_1} \quad (6)$$

a pro velikost mikrodeformací

$$e = \frac{1 \sec_2 + 2 \sec_1}{4(\tan_1 \sec_2 + \tan_2 \sec_1)} \quad (7)$$

Z rovnice (4) nebo (5) ještě plyne grafická verze této metody – analogie Williamsonova – Hallova grafu, pro více než dvě záření

SL13

STRUCTURAL EVOLUTION IN FERROMAGNETIC SHAPE MEMORY ALLOY $\text{Co}_{38}\text{Ni}_{33}\text{Al}_{29}$

J. Kopeček¹, M. Jarošová², K. Jurek², J. Dražokoupil¹, P. Molnár¹, O. Heczko¹

¹*Institute of Physics of the AS CR, Na Slovance 2, 182 21 Praha 8, Czech Republic*

²*Institute of Physics of the AS CR, Cukrovarnická 10/112, 162 00 Praha 6, Czech Republic
kopecek@fzu.cz*

Introduction

The cobalt-based shape memory alloys (SMA) are expected to be the new kind of so-called ferromagnetic SMAs [1]; this means alloys, in which the driving force for the martensitic phase transformation (direct or reverse) or martensitic variants reorientation can be the external magnetic field. This effect was described in stoichiometric compound Ni_2MnGa [2]. The mechanical properties of Co-Ni-Al alloys are definitely better than the properties of Ni-Mn-Ga alloys; they are harder and they have better creep and fatigue properties. But, the structure of Co-Ni-Al alloy is more complicated as compared to NiMnGa alloys. There are two phases at least, but only one of them undergoes the martensitic transformation. The role of the non-transforming phase during the transformation is not recognised yet, but its presence is suitable for the successful shape memory effect (SME). Single-phase alloys have tendency to crack before achieving a reasonable plastic deformation. The presented abstract describes the progress on the structural study.

The structure of the investigated material $\text{Co}_{38}\text{Ni}_{33}\text{Al}_{29}$ is composed of two phases – an ordered matrix (Co,Ni)Al with space group Pm3m, structure type B2, and a disordered face centred cubic cobalt solid solution with space group Fm3m, structure type A2 [3], Fig. 1. The B2 phase matrix undergoes martensitic transformation into the tetragonal L0_1 structure (space group P4/mmm). The transformation mechanism is very similar to the Ni-Al alloy including precursors, tweed structure and softening of the phonon modes [4]. According to the phase diagram L1_2

$$\cos D^{-1} = 4e \sin \quad (8)$$

Když tedy vyneseme závislost $\cos y$ na x , dostaneme přímkou se směrnici D^{-1} , která na ose y vytíná úsek $4e \sin$.

References

1. H.P. Klug & L.E. Alexander, X-Ray Diffraction Procedures for Polycrystalline and Amorphous Materials. New York 1974. Wiley, 2nd ed.
2. A. Guinier, X-Ray Diffraction. San Francisco and London 1963. Freeman.
3. W.A. Wood, Nature, 151 (1943) 585.
4. A. Kochanovská, Strukturní rentgenografie, Praha 1964. SNTL.

Poděkování

Tato práce vznikla v rámci realizace projektu Akademie věd České republiky - KAN 300100801.

structure (Co,Ni)₃Al (space group Fm3m) exists in samples with sufficient amount of nickel. In our samples, this phase is observed under special kinetic conditions.

The structure analysis was performed mainly using analytical electron microscopy as our samples are usually directionally crystallized structures with extremely large/coarse grains. The set of the in-situ measurements on powders was performed on synchrotron source BESSY II in HZB Berlin.

Crystal growth

In order to study and to apply ferromagnetic shape memory effect (FSME), it is very convenient to have single-crystalline samples. The single-crystals for our study were prepared using vertical floating-zone method and Bridgman method. The structure and composition of the as-grown samples were published in Refs [5, 6]. The findings from the crystal growth study can be summarized in the points:

1. The samples grown with a growth rate of 17 mm h^{-1} or lower have tendency to get splitted into a two-phase mantle (B2 matrix plus A2 interdendritic precipitates) and a single-phase (only B2) core. Such structures have tendency to crack during cutting and polishing.

2. The composition of the matrix and precipitates seems to be stable within three categories: Floating-zone sample; Bridgman sample grown with a growth rate of 17 mm h^{-1} and Bridgman samples grown with a growth rate higher than 17 mm h^{-1} . Both phases in respective categories have the same composition. The last category appears to be interesting for our investigation, since a variation of the

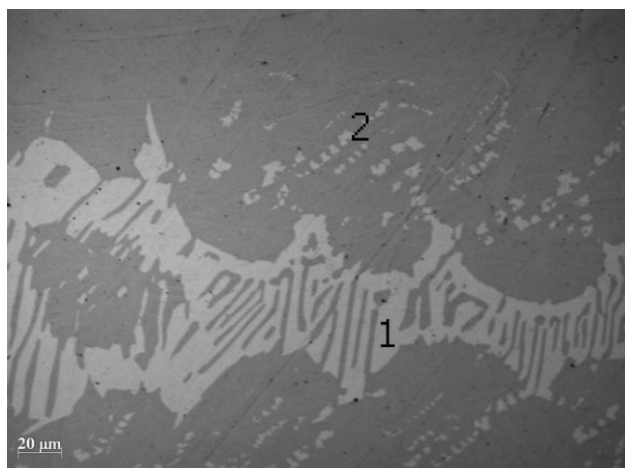


Figure 1. The structure of the samples grown with a growth rate of 38 mm h^{-1} in light microscope metallography. The precipitates marked 1 are interdendritic A2 fcc cobalt solid solution particles. The precipitates marked 2 are $L1_2$ ordered precipitates of the phase $(\text{Co,Ni})_3\text{Al}$.

chemical composition along the Bridgman crystal is realized through the change of the A2/B2 phases ratio.

3. The ordered $L1_2$ phase $(\text{Co,Ni})_3\text{Al}$ appears in the Bridgman crystals grown with a growth rate lower than 38 mm h^{-1} . It forms thin precipitates in a vicinity to A2 interdendritic precipitates. Its role in martensitic transformation is still unknown, Fig. 1.

Sample annealing

A kind of metastable (quenched) equilibrium is necessary for the SME performance in these alloys. It was described just as quick cooling after homogenization annealing in literature, but significant changes are observed mainly in the matrix [7]. Nanoprecipitates of various phases are created which can support spreading of the habit plane of martensite. The fcc and hcp cobalt solid solution precipitates with a diameter below 100 nm were observed in samples grown with a growth rate 28 and 38 mm h^{-1} . [8, 9]. Generally, the role of particular nanoprecipitates in the quenched matrix is not known [7].

A set of various annealing temperatures was employed. All samples were quenched to the ice-cold water. The temperature of $1350 \text{ }^\circ\text{C}$ leads to the dissolving of the interdendritic precipitates of the A2 (fcc cobalt) phase, but the true temperature of dissolving is lower, probably close to $1300 \text{ }^\circ\text{C}$, as was observed. The melting of the two-phase structure damages the SME. The samples showing the superelasticity (stress induced martensitic transformation) have a two-phase structure.

Past works [10] reported quite high temperatures of the martensitic transformation, but we observed $M_s \sim -73 \text{ }^\circ\text{C}$, which does not depend on the annealing temperature in the interval from $1250 \text{ }^\circ\text{C}$ up to $1350 \text{ }^\circ\text{C}$. The hysteresis of the martensitic transformation enlarges with lowering of the annealing temperature. Although the martensitic transformation takes place at temperatures below $-73 \text{ }^\circ\text{C}$, pinned martensitic structures were observed in various samples. The lamellae were pinned either by concave A2 interdendritic precipitates or by a special shape of the sam-

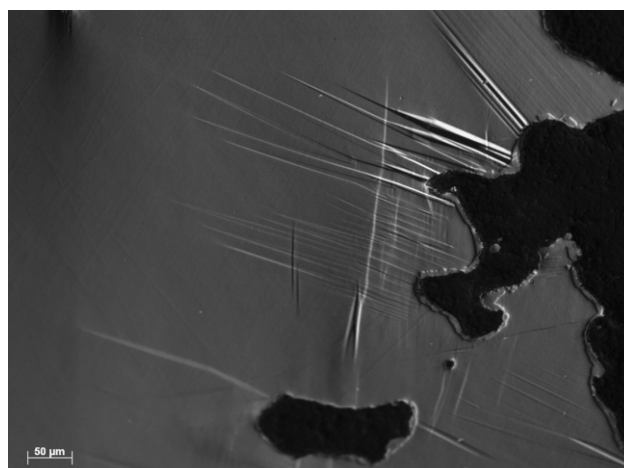


Figure 2. The sample annealed at $1250 \text{ }^\circ\text{C}$ for 1 h and quenched to the ice-cold water. Some trapped martensitic lamellae remain in special geometry of the sample up to room temperature.

ple – thin edge, Fig. 2. The details of the pinning configuration are under examination.

References

1. Heczko O., Scheerbaum N., Gutfleisch O., *Magnetic Shape Memory Phenomena*, in *Nanoscale Magnetic Materials and Applications*, edited by J.P. Liu et al. (Springer Science+Business Media, LLC), 2009, pp. 14-1.
2. Heczko O, Sozinov A, Ullakko K, *IEEE Trans. Magn.*, **36**, (2000), 3266-3268.
3. M. Hubert-Protospescu, H. Hubert, *Aluminium-cobalt-nickel ternary alloys: a comprehensive compendium of evaluated constitutional data and phase diagram. Vol. 4: Al-Cd-Ce to Al-Cu-Ru*, edited by G. Petzow & G. Effenberg (Weinheim: VCH) 1991, pp. 234.
4. Y. Murakami, D. Shindo, K. Oikawa, R. Kainuma, K. Ishida, *Acta Mater.*, **50**, (2002), 2173.
5. J. Kopeček, K. Jurek, M. Jarošová, et al., *IOP Conf. Sci.: Mater. Sci. Eng.*, **7**, (2010), 012013.
6. J. Kopeček, S. Sedláková-Ignácová, K. Jurek, M. Jarošová, J. Drahokoupil, P. Šittner, V. Novák: *Structure development in $\text{Co}_{38}\text{Ni}_{33}\text{Al}_{29}$ ferromagnetic shape memory alloy*, 8th European Symposium on Martensitic Transformations, ESOMAT 2009, edited by Petr Šittner, Václav Paidar, Luděk Heller, Hanuš Seiner, 2009, article No. 02013.
7. Yu. I. Chumlyakov, I. V. Kireeva, E. Yu. Panchenko, E. E. Timofeeva, Z. V. Pobedennaya, S. V. Chusov, I. Karaman, H. Maier, E. Cesari and V. A. Kirillov, *Russ. Phys. J.*, **51**, (2008), 1016.
8. B. Bartova, D. Schryvers, Z. Q. Yang, S. Ignacova, P. Šittner, *Scripta Mater.*, **57**, (2007), 37.
9. B. Bartova, N. Wiese, D. Schryvers, N. J. Chapman, S. Ignacova, *Acta Mater.*, **56**, (2008), 4470.
10. K. Oikawa, L. Wulff, T. Iijima, F. Gejima, T. Ohmori, A. Fujita, K. Fukamichi, R. Kainuma, K. Ishida, *Appl. Phys. Lett.*, **79**, (2001), 3290.

Authors would like to acknowledge the financial support from the Grant Agency of the AS CR project IAA2001 00902 and Czech Science Foundation projects 101/09/0702 and P107/10/0824.